

Single-Molecule Detection of Airborne Singlet Oxygen

Kazuya Naito, Takashi Tachikawa, Shi-Cong Cui, Akira Sugimoto, Mamoru Fujitsuka, and Tetsuro Majima*

The Institute of Scientific and Industrial Research (SANKEN), Osaka University, Mihogaoka 8-1, Ibaraki, Osaka 567-0047, Japan

Received September 19, 2006; E-mail: majima@sanken.osaka-u.ac.jp

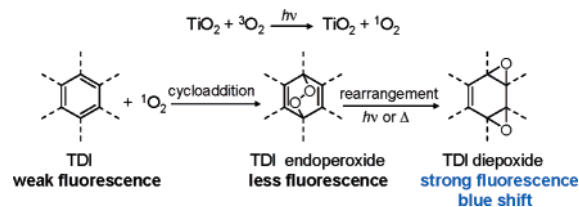
The singlet oxygen ($^1\text{O}_2$) molecule is an important reactive oxygen species in atmospheric, biological, and therapeutic processes and is also used as a reagent in organic synthesis.¹ Recently, it has been reported that $^1\text{O}_2$ molecules are directly or indirectly generated via energy or electron-transfer reactions between oxygen molecules in the ground state ($^3\text{O}_2$) and semiconductor nanomaterials, such as silicon,² titanium dioxide (TiO_2),³ and CdSe quantum dots.⁴ Although the generation yields of $^1\text{O}_2$ molecules from these materials in solution are much lower than those from organic dye sensitizers,⁵ the materials will be the basis of newly emerging nanobiotechnologies because of their temporal stability.⁶ Thus, much would be gained if tenuous $^1\text{O}_2$ molecules in air, solution, and biological systems could be directly monitored with both time and spatial resolutions.

In this Communication, we report the single-molecule detection of an airborne $^1\text{O}_2$ molecule diffused from the surface of TiO_2 nanoparticles using total internal reflection fluorescence microscopy (TIRFM).⁷ Although $^1\text{O}_2$ molecules are believed to be generated during the TiO_2 photocatalytic reactions and the formation mechanism has been proposed (see Supporting Information, S1),³ there is no direct evidence to support the diffusion from the surface to the gas phase. Our strategy to detect $^1\text{O}_2$ molecules at the single-molecule level is summarized in Scheme 1. Terrylenediimide (TDI, the molecular structure, spectral characteristics, and the reaction rate with $^1\text{O}_2$ in bulk solution are given in Supporting Information, S2)⁸ is used as the $^1\text{O}_2$ sensor. A single TDI molecule is oxidized by a single $^1\text{O}_2$ molecule to form a less fluorescent endoperoxide and successively a strongly fluorescent diepoxide with a spectral blue-shift that is easily detected upon 532-nm laser excitation. A similar structural change and spectral shift have been reported for a single terylene molecule doped in the *p*-terphenyl crystal.⁹

The experimental setup is based on TIRFM using an Olympus IX71.¹⁰ The sample is composed of a TDI-coated coverslip and the TiO_2 film-coated slide glass with an intervening gap (12.5–2000 μm). First, a coverslip was spin-coated with a toluene solution of poly(methylmethacrylate) (PMMA) (10 g dm^{-3}) and subsequently with a chloroform solution of TDI (3 nM). There are two roles for this underlying PMMA, as follows: (i) protecting TDI from the self-sensitization due to excess $^3\text{O}_2$ molecules and (ii) excluding the oxidation of TDI due to the photocatalytically generated radicals, such as $\cdot\text{OH}$ or $\cdot\text{HO}_2$,¹¹ because PMMA can react with the radicals^{12a} but not extensively with $^1\text{O}_2$.^{12b} A TiO_2 film was irradiated with UV light (365 nm) to generate airborne $^1\text{O}_2$ molecules. The cycloaddition reaction between the TDI and airborne $^1\text{O}_2$ was observed at the coverslip–air interface using TIRFM (see Supporting Information, S2).

Figure 1 shows the single-molecule fluorescence images observed before (A) and after (B) UV irradiation of the TiO_2 film for 5 min. Before UV irradiation, only a few fluorescent spots were observed owing to the weak fluorescence of the TDI excited at 532 nm. Because of the lack of sensitivity against the weak fluorescence, almost

Scheme 1. Single-Molecule Detection of Airborne $^1\text{O}_2$ with TDI



all TDIs cannot be recognized in Figure 1A. Interestingly, after UV irradiation, bright fluorescent spots emerged around the UV-irradiated region as described by the white circles in Figure 1. This observation is consistent with the fact that the bleaching of dyes occurred around the UV-irradiated region, as previously reported.¹⁰

These fluorescent spots would arise from the TDI diepoxide, which is formed by the cycloaddition reaction between the TDI and airborne $^1\text{O}_2$ generated during the TiO_2 photocatalytic reactions. To clarify the formation of the TDI diepoxide, the single-molecule fluorescence spectra were measured for each spot before and after the UV irradiation. The spectra are shown in Figure 2A. The black line is a typical single-molecule fluorescence spectrum before UV irradiation. The observed spectrum, which has a peak wavelength about 670 nm, is very similar to that measured in CHCl_3 solution (blue line). However, its fluorescence intensity is too weak to be precisely detected in the images as already mentioned (Figure 1A). The red line is a typical single-molecule fluorescence spectrum after UV irradiation. Compared to that before UV irradiation, it was found that the spectrum after UV irradiation is blue-shifted by approximately 70 nm and has a strong fluorescence intensity. Thus, the bright fluorescent spots shown in Figure 1B should be the TDI diepoxide, similar to a terylene molecule reported by Basché et al.⁹ The few bright spots in Figure 1A also have a blue-shifted spectrum arising from the TDI diepoxide due to the self-sensitization. The fact that the TDI diepoxide shows a strong fluorescence intensity, when compared with that of TDI, is explained as the increase in the absorbed photon due to the blue shift of the absorption spectrum (see Supporting Information, S3).

Figure 2B shows the histogram of the peak wavenumber of the fluorescence spectra before (upper panel) and after (lower panel)

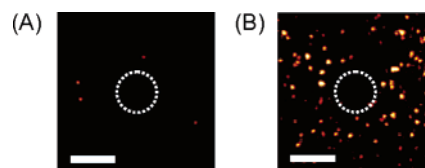


Figure 1. Fluorescence images of single TDIs spin-coated on the PMMA-coated coverslip before (A) and after (B) UV irradiation for 5 min (scale bars are 10 μm). The intervening gap is 12.5 μm . The bright spots correspond to the blue-shifted, TDI diepoxide. The UV irradiation area is inside the white circle in the images. The absence of dyes at the center of the image after UV irradiation is due to the bleaching of dyes caused by the direct UV irradiation.

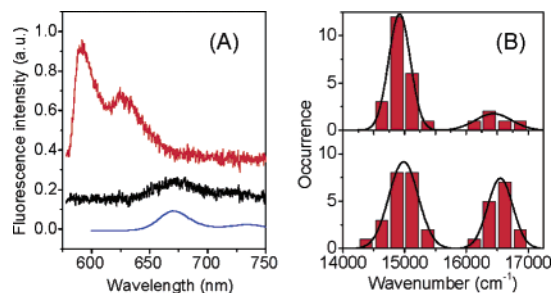


Figure 2. (A) Typical single-molecule fluorescence spectra of TDI before (black) and after (red) UV irradiation for 5 min. The intervening gap is 12.5 μm . The fluorescence spectra were obtained from excitation at 532 nm and cut below 580 nm by a long-pass filter on the blue edge. The fluorescence spectrum of TDI measured in CHCl_3 solution is shown for comparison (blue). (B) Histogram of the peak wavenumber of the spectra observed before (upper panel) and after (lower panel) UV irradiation for 2 min. Solid lines indicate Gaussian distributions fitted with the histograms.

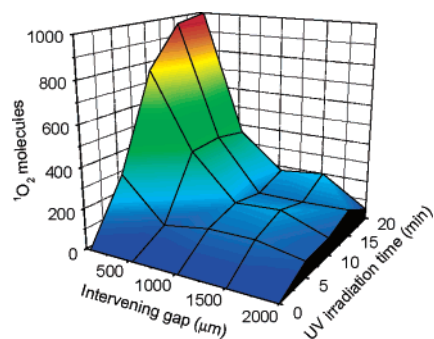


Figure 3. The spatial and temporal distributions of $^1\text{O}_2$ molecules diffused from the surface of TiO_2 film. The observation region is $70 \times 70 \mu\text{m}^2$. The intervening gaps are 50, 500, 1000, 1500, and 2000 μm .

UV irradiation for 2 min. It should be noted that the histogram of the peak wavenumber of the spectra observed during UV irradiation indicates two maxima around 15000 and 16500 cm^{-1} , which are assigned to the parent TDI and TDI diepoxide, respectively. After UV irradiation, the number of TDI diepoxides, that is, the number of $^1\text{O}_2$ molecules, clearly increased. It should also be noted that no further spectral blue shift due to multiple attacks of $^1\text{O}_2$ was observed in the present wavelength range. Therefore, the bright spots in the fluorescence images can be regarded as a signal of single $^1\text{O}_2$ molecules. This enables us to count the $^1\text{O}_2$ molecules, although a part of the $^1\text{O}_2$ molecules might be deactivated in the PMMA film.

As a control experiment, four experiments have been performed as follows: (i) in the absence of the TiO_2 film, (ii) in an argon atmosphere, (iii) in the presence of a known $^1\text{O}_2$ quencher, 1,4-diazabicyclo[2.2.2]octane (DABCO),^{12b} and (iv) using the “top-coat” PMMA sample, where TDI is spin-coated prior to PMMA. In all the control experiments, the increase in the TDI diepoxide was significantly suppressed. The reasons are that (i) TiO_2 is essentially required in the photocatalytic reactions and the self-sensitization of TDI is ineffective, (ii) $^3\text{O}_2$ molecules are required for the formation of $^1\text{O}_2$ molecules, (iii) DABCO quenches $^1\text{O}_2$ molecules, and (iv) the “top-coat” PMMA film protects TDI from the approach of airborne $^1\text{O}_2$ molecules (see Supporting Information, S4).

Using this $^1\text{O}_2$ nanosensor, the spatial and temporal distributions of single airborne $^1\text{O}_2$ molecules diffused from the TiO_2 film have been successfully investigated. This result is shown in Figure 3. Several dozen $^1\text{O}_2$ molecules are detected even at the intervening gap of 2000 μm . To the best of our knowledge, this is the first example of the single-molecule detection of molecules traveling such a long distance in ambient air.¹³ The quantitative analysis

enables us to estimate the generation efficiency of airborne $^1\text{O}_2$ molecules during the TiO_2 photocatalytic reactions. The number of airborne $^1\text{O}_2$ molecules near the TiO_2 film was tentatively estimated by extrapolating the intervening gap to zero. Considering the estimated values and the number of photons absorbed by the TiO_2 film, the generation efficiency of the airborne $^1\text{O}_2$ molecules during UV irradiation of 5, 10, 15, and 20 min are determined to be 11, 9.7, 8.4, and 6.5×10^{-9} , respectively (see Supporting Information, S2). Assuming that the generation efficiency of $^1\text{O}_2$ on the surface does not depend on the UV irradiation time, the decrease in the generation efficiency of the airborne $^1\text{O}_2$ would be due to the numerical saturation of the sensing TDI molecules and the degradation of the TDI diepoxide.

In conclusion, we have successfully detected airborne $^1\text{O}_2$ molecules generated during the TiO_2 photocatalytic reactions at the single-molecule level. This is a modern version of the Kautsky experiment.^{1a} The present nanosensor using single TDI molecules, which has a detectable number of about 1000 $^1\text{O}_2$ molecules in a $70 \times 70 \mu\text{m}^2$, can easily detect the single $^1\text{O}_2$ molecule at the distance of $>1000 \mu\text{m}$ from the place of its creation in ambient air. This ultimate analysis of $^1\text{O}_2$ molecules will be a powerful tool in many fields, such as the material and biological sciences.

Acknowledgment. This work has been partly supported by a Grant-in-Aid for Scientific Research (Project 17105005, Priority Area (417), 21st Century COE Research, and others) from the Ministry of Education, Culture, Sports, Science and Technology (MEXT) of Japanese Government.

Supporting Information Available: Short historical review of $^1\text{O}_2$ detection and photocatalytic reaction schemes (S1), experimental and analytical details (S2), quantum calculations (S3), and control experiments (S4). This material is available free of charge via the Internet at <http://pubs.acs.org>.

References

- (1) (a) Kautsky, H. *Trans. Faraday Soc.* **1939**, *35*, 216–219. (b) Wasserman, H. H.; Murray, R. W. *Singlet Oxygen*; Academic Press: New York, 1979. (c) Schweitzer, C.; Schmidt, R. *Chem. Rev.* **2003**, *103*, 1685–1757. (d) Dolmans, D. E. J. G. J.; Fukumura, D.; Jain, R. K. *Nat. Rev. Cancer* **2003**, *3*, 380–387.
- (2) Kovalev, D.; Fujii, M. *Adv. Mater.* **2005**, *17*, 2531–2544.
- (3) For example, (a) Tatsuma, T.; Tachibana, S.; Fujishima, A. *J. Phys. Chem. B* **2001**, *105*, 6987–6992. (b) Nosaka, Y.; Daimon, T.; Nosaka, A. Y.; Murakami, Y. *Phys. Chem. Chem. Phys.* **2004**, *6*, 2917–2918. (c) Hirakawa, K.; Hirano, T. *Chem. Lett.* **2006**, *35*, 832–833.
- (4) Samia, A. C. S.; Chen, X.; Burda, C. *J. Am. Chem. Soc.* **2003**, *125*, 15736–15737.
- (5) For example: Bonnett, R. *Chem. Soc. Rev.* **1995**, *24*, 19–33.
- (6) (a) Fujishima, A.; Rao, T. N.; Tryk, D. A. *J. Photochem. Photobiol. C: Photochem. Rev.* **2000**, *1*, 1–21. (b) Paunesku, T.; Rajh, T.; Wiederecht, G.; Maser, J.; Vogt, S.; Stojićević, N.; Protić, M.; Lai, B.; Oryhon, J.; Thurnauer, M.; Woloschak, G. *Nature Mater.* **2003**, *2*, 343–346. (c) Clarke, S. J.; Hollmann, C. A.; Zhang, Z.; Suffern, D.; Bradforth, S. E.; Dimitrijević, N. M.; Minarik, W. G.; Nadeau, J. L. *Nature Mater.* **2006**, *5*, 409–417.
- (7) Funatsu, T.; Harada, Y.; Tokunaga, M.; Saito, K.; Yanagida, T. *Nature* **1995**, *374*, 555–559.
- (8) (a) Holtrup, F. O.; Müller, G. R. J.; Quante, H.; De Feyter, S.; De Schryver, F. C.; Müllen, K. *Chem.–Eur. J.* **1997**, *3*, 219–225. (b) Cotlet, M.; Vosch, T.; Habuchi, S.; Weil, T.; Müllen, K.; Hofkens, J.; De Schryver, F. J. *Am. Chem. Soc.* **2005**, *127*, 9760–9768.
- (9) Christ, T.; Kulzer, F.; Bordat, P.; Basché, T. *Angew. Chem., Int. Ed.* **2001**, *40*, 4192–4195.
- (10) Naito, K.; Tachikawa, T.; Fujitsuka, M.; Majima, T. *J. Phys. Chem. B* **2005**, *109*, 23138–23140.
- (11) Kubo, W.; Tatsuma, T.; Fujishima, A.; Kobayashi, H. *J. Phys. Chem. B* **2004**, *108*, 3005–3009.
- (12) (a) Linden, L. A.; Rabek, J. F.; Kaczmarek, H.; Kaminska, A.; Scoponi, M. *Coord. Chem. Rev.* **1993**, *125*, 195–218. (b) Ogilby, P. R.; Iu, K.; Clough, R. L. *J. Am. Chem. Soc.* **1987**, *109*, 4746–4747.
- (13) (a) The average value of the square of distance d , which a molecule travels during time τ , depends on its D value according to $d^2 = 6D\tau$. The diffusion length of $^1\text{O}_2$ is estimated to be 3.5 mm with $D = 0.18 \text{ cm}^2 \text{ s}^{-1}$ and $\tau = 70 \text{ ms}$.^{1c,13b} (b) Massman, W. J. *Atmos. Environ.* **1998**, *32*, 1111–1127.

JA066739B